Accepted Manuscript


# Smart, Biocompatible, Responsive Surfaces on pH, Temperature and Ionic Strength of Titanium Oxide and Niobium Oxide with Polymer brushes of Poly(acrylic acid), Poly(N-isopropylacrylamide) and Poly([2-(methacryloyloxy)ethyl] trimethylammonium chloride)

Nikos Politakos, Eleftheria Diamanti, Sergio E. Moya

PII: S0014-3057(18)32255-9
DOI: https://doi.org/10.1016/j.eurpolymj.2019.01.018
Reference: EPJ 8798

To appear in: *European Polymer Journal*

Received Date: 13 November 2018
Revised Date: 11 December 2018
Accepted Date: 7 January 2019

Please cite this article as: Politakos, N., Diamanti, E., Moya, S.E., Smart, Biocompatible, Responsive Surfaces on pH, Temperature and Ionic Strength of Titanium Oxide and Niobium Oxide with Polymer brushes of Poly(acrylic acid), Poly(N-isopropylacrylamide) and Poly([2-(methacryloyloxy)ethyl] trimethylammonium chloride), *European Polymer Journal* (2019), doi: https://doi.org/10.1016/j.eurpolymj.2019.01.018

# Smart, Biocompatible, Responsive Surfaces on pH, Temperature and Ionic Strength of Titanium Oxide and Niobium Oxide with Polymer brushes of Poly(acrylic acid), Poly(N-isopropylacrylamide) and Poly([2-(methacryloyloxy)ethyl] trimethylammonium chloride)

**Nikos Politakos[a,b*], Eleftheria Diamanti[a,c] & Sergio E. Moya[a]**

[a]*Soft Matter Nanotechnology, CIC biomaGUNE, Paseo Miramón 182 C, 20014 Donostia-San Sebastian, Spain.*
[b]*POLYMAT and Departamento de Química Aplicada, Facultad de Ciencias Químicas, University of the Basque Country UPV/EHU, Joxe Mari Korta Center, Avda. Tolosa 72, 20018 Donostia—San Sebastian, Spain.*
[c]*CIC nanoGUNE, Tolosa Hiribidea 76 E-20018, Donostia – San Sebastian, Spain.*

[*]Corresponding Author: nikolaos.politakos@ehu.eus

**Abstract:** Titanium and Niobium oxide are metallic surfaces used as biomaterials due to their biocompatibility. Their improvement is very important in order to create smart surfaces in terms of responsiveness, with polymer brushes that have a switchable behavior in external stimulus of pH, temperature and ionic strength. The combination with poly(acrylic acid) - PAA, Poly(N-isopropylacrylamide) - PNiPAM and Poly([2-(methacryloyloxy)ethyl] trimethylammonium chloride) – PMETAC polymer brushes as long as their evaluation in biocompatibility and adhesion with cells can lead to smart surfaces that can be used as biomaterials.

**Highlights**

- Responsive polymer brushes grafted from $TiO_2$ and NbO surfaces
- AFM (liquid-dry) and contact angle characterization to show responsiveness
- Responsive to pH, ionic strength and temperature
- Increased biocompatibility of preosteoblasts at polymer brushes samples
- Confocal microscopy reveals cellular adhesion

**Keywords:** responsive surfaces; titanium oxide; niobium oxide; polymer brushes; AFM; biocompatibility

## 1. Introduction

Polymeric synthesis of materials is very important when new challenges demand advanced applications in technologies. There are numerous of classes of polymeric materials, with one of the most promising being "*polymer brushes*". The area is not new and there are quite a few references of polymer brushes composed from different polymers and architectures as long as different ways of synthesis of those materials. Nevertheless, new applications are evolving demanding new materials. Polymer brushes are potential smart materials showing reversible changes in response to small changes e.g., temperature, presence of salts, solvent, pH, electric potential etc. [1,2]. The physicochemical properties, shape, conformation and morphology of polymers brushes can be changed, leading to a plethora of applications. Their advantage, when compared to other modification methods (e.g. self-assembled monolayers) is that they exhibit chemical and mechanical robustness and high diversity in synthesis (different monomers, architectures, thickness, density, molecular characteristics and functionality) [2]. The use of polymer brushes for tailoring the surface properties; friction, resistance, wettability and biocompatibility of a variety of surfaces offer to those surfaces new properties and applications [2]. The reversible behavior that is derived from the functional groups, the stretched conformations in order to minimize segment-segment interactions and their different morphologies are what makes them attractive for potential use in different applications [3–5]. Polymer brushes on surfaces can be used in different applications such as: responsive interfaces, drug delivery, release systems, sensors, coatings, composites, applications that require cell adhesion, photo controlled surfaces, bioelectronic systems, thermoresponsible surfaces, organic electronic devices, catalysis and biocatalysis and protein fouling [1,6–9].

Polymer brushes can be synthesized with many known polymerization techniques, such as ATRP, anionic, NMP or RAFT. The strategy for fabricating the brush can be differentiated in two major ways "from" and "to". Among the different polymerization techniques, RAFT is becoming more attractive due to the control over molecular characteristics, broad range of functional monomers (when compared to other techniques), compatibility with different reaction media (organic and aqueous) and possibility of adoption from the industry [10]. Especially high temperatures are avoided as in the case of the classical NMP and non-toxic metals are required as in ATRP [8]. Among the strategies "from" and "to", better results are obtained with the "from", giving stable brushes with control over thickness and density [11,12].

Even though there are a lot of different polymers that can be synthesized as brushes from a surface, there are some that have gain attention due to their properties in switching behavior. Polyelectrolyte brushes have drawn attention due to their anisotropic nature and solution properties [13], the biocompatibility and non-biofouling ability [14] while the different bonding and adhesion depends on the aquatic environment [15]. These polymer brushes, based on their properties can lead to applications where a stimuli material

with switching behavior is needed [3,4]. Of equal importance is the use of thermoresponsive polymers; their switching behavior is derived from changes of their conformation due to alteration of temperature such as PNiPAM [16–18].

The modification of metal surfaces with polymer brushes is an evolution in the area of biomaterials since by using the good properties of metals (e.g. mechanical superiority) and the antifouling properties or the selective absorption of the polymers great advances can be achieved [19–24]. Niobium (Nb) and Titanium (Ti) are two metallic surfaces already used. Both of those materials have very interesting properties, such as resistance to corrosion (their corrosion products are present in the tissue not as ions but as stable oxides), biocompatibility, bioactivity, no release of harmful metals and prevent exchange of electrons (so less redox reactions) [25–29]. In order to improve their properties, diminish the nonspecific protein adsorption and cell adhesion, polymer brushes can be used as an effective method for surface modification. This implies that these materials can be used in numerous of applications such as in orthopedic and dental implants, tissue engineering, biosensors and diagnostics [30–33]. In literature, some examples of polymer brushes synthesis from metal oxides and especially from Ti can be found [34].

The basic aim of this study is to synthesize polymer brushes using poly(acrylic acid) PAA, poly(N-isopropylacrylamide) PNiPAM and Poly[(2(Methacryloyloxy)Ethyl) TrimethylammoniumChloride] PMETAC, from metal oxide surfaces of niobium (NbO) and titanium ($TiO_2$). The polymer brushes grafted from $TiO_2$ and NbO will be examined for their switching ability in different conditions, such as pH, temperature and salt concentration and for their biocompatibility by studying the cellular adhesion via XPS, AFM, contact angle and confocal microscopy.

## 2. Experimental Part

### 2.1 Materials

[2-(Methacryloyloxy)ethyl] trimethylammonium chloride (*METAC*) solution 80 wt. % in $H_2O$, acrylic acid (*AA*), anhydrous, contain 200 ppm MEHQ as inhibitor (99 %) and N-Isopropylacrylamide (*NiPAM*) (97 %) were purchased from Aldrich. The initiators: 4,4′-Azobis(4-cyanovaleric acid) (*CVA*), (≥98 %) as well purchased from Aldrich. As change transfer agent (*CTA*) cyanomethyl [3-(trimethoxysilyl)propyl] trithiocarbonate (95 % - Aldrich) was used. Finally as a solvent *N*,*N*-Dimethylformamide (*DMF*), (anhydrous, 99.8 %-Aldrich) was used and nanopure water for the synthesis of PMETAC. Phosphate buffer saline 10x (PBS) and formaldehyde solution 37 % and fluoromount aqueous mounting medium, fibronectin from human plasma and minimum essential medium (MEM) were purchased from Sigma-Aldrich. Fetal bovine serum (FBS) was provided by Fisher. Actin Cytoskeleton and Focal Adhesion Staining Kit (FAK100) was obtained from Millipore.

### 2.2 Synthesis of polymer brushes grafted "from"

The first step for the polymerization process was the immobilization of the CTA onto the metallic surfaces of $TiO_2$ or NbO. These were prepared by spattering Ti or Nb over a glass slide whose preparation was done by depositing in a reactive configuration applying a RF power of 100 W to the Nb or Ti target at gas mixtures of Ar/O 50/5. The glass slides were cut in appropriate sizes and were placed in $UV/O_3$ chamber for 30 min approximately in order to remove any organic material. CTA has three -S- groups in the structure with a silane that can be bonded to the oxide of the metallic surface as reported in the literature [9]. By this way, the CTA provides to the structure both a silane to bond onto the surface and a trithiocarbonate moiety where the polymerization can initiate. So by just one step the CTA is grafted onto the surface. CTA was dissolved at DMF at a 50 mM (samples abbreviated 1 for $TiO_2$ & 3 for NbO) and 100 mM (samples abbreviated 2 for $TiO_2$ and 4 for NbO) concentrations. Substrates were left in the CTA solution under inert atmosphere ($N_2$) to react overnight at room temperature. Subsequently, the substrates were slightly sonicated in ethanol in order to remove unreacted species. An XPS characterization was carried out in order to verify the presence of the -S- groups onto the Au surface.

CVA was used as initiator for the polymerization due to its hydrophilic character. For the homopolymerization process a solution of the monomer, initiator and solvent was purged (DMF, for the PNiPAM or PAA and DMF/$H_2O$, 60:40 v/v for the PMETAC) under inert atmosphere for several hours at a total concentration of 5 % w/v. The polymerization time was set to 15 h for all monomers at 70 $^oC$ under inert atmosphere. After polymerization, the substrates were put into a sonication bath for a few minutes to remove unreacted species. Samples with **PAA** are abbreviated as *A*, with **PNiPAM** as *N* and with **PMETAC** as *M*. The number 1 to 4 is referred to the concentrations and the type of metallic surface (1: 50 mM – $TiO_2$, 2: 100 mM – $TiO_2$, 3: 50 mM – NbO & 4: 00 mM – NbO).

As already mentioned the different ratios play very important role [10], for the [M]/[CTA] and the [CTA]/[I], are very important since through them the degree of polymerization (and the molecular weight) as long as the functionality of the chains can be controlled. So, the aim here was to retain the first ratio as high as possible for the polymer to grow ([M]/[CTA]=10). The ratio of the [CTA]/[I] was also low in order to avoid too many chains with the initiator part as free polymer in the solution ([CTA]/[I]=10. In Figure 1 it can be observed the followed synthetic route.

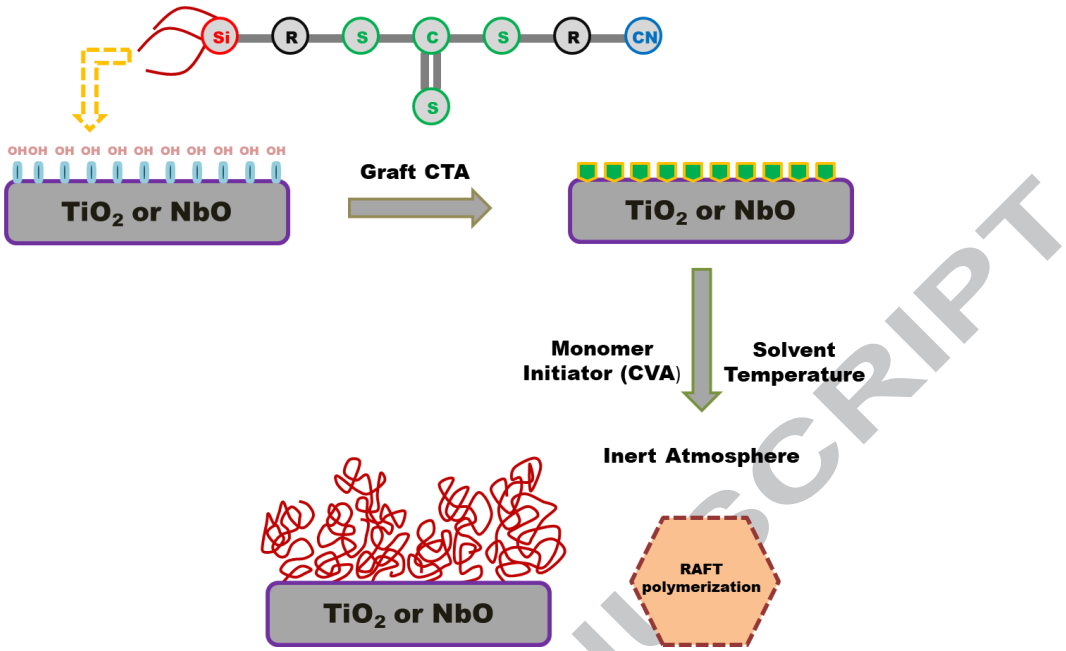


**Figure 1:** Schematic representation of the synthesis of polymer brushes grafted from $TiO_2$ or NbO.

### 2.3 Characterization Methods

XPS measurements were conducted in order to have a better knowledge about the structure of the copolymers and to recognize specific elements of the blocks: F for the PPFDA, S for the PSPM and N for the PMETAC. Based on these elements the ratios of hydrophobic to hydrophilic blocks were determined. Surface analysis via XPS was performed in a SPECS SAGE HR 100 system spectrometer. The x-ray source employed for this analysis was a Mg Kα (1253.6 eV) operated at 12.5 kV and 250 W. The take-off angle was fixed at 90º and the analysis was conducted at a pressure of ~$10^{-8}$ Torr. Survey spectra were obtained with pass energy of 30 eV.

The morphological characterization of the copolymers was done using AFM with a Veeco Multimode atomic force microscope attached to a Nanoscope V controller. The tips for the AFM were from Bruker and the model was TESP-V2 with k: 42 N/m. For the measurements in liquid, AFM tips from Bruker were use in water solution with 10 mM of NaCl, the model was DNP-S 10 with k: 0.24 N/m.

Contact angle measurements were done with a DSA100 Contact Angle Measuring System with a DSA100 control from the Kruss Company. Measurements were conducted at room temperature approaching a droplet of volume of 3 µl at 500 µl/min speed. Before each measurement the surfaces were left in a specific solution (solvent, pair of solvents, solution of different salts or aquatic solutions of different pH). After a small a period of time the surfaces treated with solvents were left to evaporate, in addition to the other treatment (salts or different pH), where the surfaces were dried under nitrogen flow. Subsequently the surfaces were used for the contact angle measurements; for each sample, three

measurements were done in order to have a reproducibility of the results. Between the different solutions, each surface was first left in water of pH 7 to bring the brushes in the initial state before each measurement.

For the cellular adhesion studies, MC-3-T3 murine osteoblasts eukaryotic cell line was cultured and incubated at 37 ºC in a 5 % $CO_2$ and 97 % humidified atmosphere, in a-MEM medium supplemented with 10% FBS, 1 % penicillin-streptomycin and 2 mM L-glutamine. When the cultured cells reached a confluence of 70 % they were trypsinized. For cell adhesion studies the pretreated ($TiO_2$, NbO etc.) surfaces were placed into tissue culture petri dishes (d=35 mm) and UV-sterilized for 1 hour. 100 000 cells were seeded into each petri dish. 24 hours later the cells were rinsed with PBS and fixed with formaldehyde 3.7 %.

For the cell Immunostaining, Vinculin, actin and cell nucleus of MC-3-T3 preosteoblasts were fluorescently stained in order to study the cell adhesion on $TiO_2$ and NbO surfaces functionalized with polymer brushes; PAA (A1-4), PNIPAN (N1-4) and PMETAC (M1-4). Fixed cells were permeabilized at room temperature with 0.1 % Triton X-100 in PBS for 5 min. After washing with PBS cells were incubated during 30 min with a blocking solution, 1 % BSA in PBS. Anti-vinculin antibody was diluted in the blocking solution and incubated for 1 h. After three washing steps with PBS the anti-mouse IgG-FITC conjugated antibody was diluted together with the TRITC-conjugated phalloidin in PBS and incubated simultaneously for 45 min for double labeling. Finally, the cells were incubated with DAPI diluted in PBS for 3 min for nucleus staining. The samples were washed and mounted on a slide using fluoromount aqueous mounting medium and observed by Confocal Microscope (Zeiss LSM510).

## 3. Results & Discussion

### 3.1 XPS

XPS measurements were conducted for the characterization of the polymer brushes grafted from the $TiO_2$ or NbO surfaces. By XPS measurements, it is possible to identify the different percentages of the elements derived from the polymer as long as the elements of CTA. For all samples, different areas were chosen for characterization and specific analysis; PNiPAM and PMETAC: C, O and N and for PAA C & O. In addition, the areas of S and Si were also scanned, for the CTA. In Figure 1, it can be seen that the CTA has 3 S and 1 Si, in its chemical structure. In Figure 2 and Table 1 the different percentages of these elements as long as the ratio between polymer/CTA and information about the molecular characteristics of the brushes can be seen. For the molecular characteristics of these samples, it is clear that the molecular weights are relatively low, especially in the case of PMETAC. PAA showed higher values (3,331 g/mol for 50 mM and 4,663 g/mol for 100 mM), where PMETAC and PNiPAM had values around 1,500-2,000 g/mol (again with the lower values being for 100Mm). Nevertheless, these polymer brushes showed a

relatively dense packing as their grafting density varies from 0.48 to 1.57 chains/nm$^2$ (Table 1). As a general comment, the grafting density on $TiO_2$ was found slightly denser than the polymer brushes prepared on NbO. In addition, concerning the polymers, PNiPAM had a denser packing, then PMETAC and finally PAA. The metallic oxide surfaces had a high coverage of the CTA and the analogies used for the polymerization gave low molecular weight polymer brushes with a relatively extend conformation and high grafting density.

**Table 1:** XPS percentages of all samples, for Ti, Nb, C, O, N, Si & S and the ration between polymer/CTA.

| Samples | S & Si (CTA) | N | O | C | Ti or Nb | Pol/CTA[a] | Polymer[b] | $M_w$ (g/mol)[c] | σ (chains/nm$^2$)[d] |
|---|---|---|---|---|---|---|---|---|---|
| **N1-$TiO_2$** | 4.6 | 2.1 | 59.1 | 18.0 | 16.3 | 3.32 | **PNiPAM-1** | 1,718 | NbO: 0.96 |
| **N2-$TiO_2$** | 2.4 | 2.8 | 54.9 | 23.0 | 16.9 | 3.66 | | | $TiO_2$: 1.29 |
| **N3-NbO** | 1.4 | 2.4 | 57.8 | 12.9 | 25.4 | 2.39 | **PNiPAM-2** | 1,411 | NbO: 1.17 |
| **N4-NbO** | 1.8 | 3.4 | 56.3 | 14.6 | 23.3 | 2.59 | | | $TiO_2$: 1.57 |
| **A1-$TiO_2$** | 8.0 | - | 55.5 | 25.0 | 11.5 | 5.78 | **PAA-1** | 4,663 | NbO: 0.48 |
| **A2-$TiO_2$** | 3.4 | - | 53.5 | 28.2 | 14.9 | 6.25 | | | $TiO_2$: 0.50 |
| **A3-NbO** | 4.7 | - | 61.9 | 15.2 | 18.2 | 4.71 | **PAA-2** | 3,331 | NbO: 0.68 |
| **A4-NbO** | 2.4 | - | 53.4 | 25.8 | 18.5 | 5.3 | | | $TiO_2$: 0.70 |
| **M1-$TiO_2$** | 1.2 | 2.5 | 54.6 | 24.5 | 17.2 | 4.06 | **PMETAC-1** | 2,022 | NbO: 0.86 |
| **M2-$TiO_2$** | 2.1 | 2.6 | 53.5 | 23.4 | 18.6 | 2.24 | | | $TiO_2$: 0.84 |
| **M3-NbO** | 1.2 | 5.6 | 58.2 | 14.9 | 20.1 | 2.16 | **PMETAC-2** | 1,768 | NbO: 1.01 |
| **M4-NbO** | 1.8 | 4.0 | 56.4 | 16.9 | 20.9 | 1.99 | | | $TiO_2$: 0.97 |

[a] The ration between polymer/CTA, was calculated from C, O & N for PMETAC and PNIAPM & C & O for PAA, as long as for the CTA the percentages of Si & S were used.
[b] The solution polymerizations for 50mM (-1) and 100 mM (-2) were performed for calculating the molecular weight.
[c] Molecular weight for the homopolymers was calculated from GPC/SEC experiments (THF, 30 $^oC$ and calibrated with PS standards) and MALDI-TOF. For PAA and PMETAC, results are from GPC and for PNiPAM from MALDI-TOF.
[d] The grafting density was calculated from the equation $\sigma = d(g/cm^3) \times L(nm) \times N_A \times 10^{-21} / M_w$. For $M_w$ were used the ones found from GPC/SEC and MALDI-TOF experiments. As for the height of the brushes, for PAA and PMETAC the height from AFM in liquid was used, where for PNiPAM the height from AFM in dry state.

The specific positions of the elements can be found in literature. In the case of *PAA* [35], the most important positions of C and O (except C-C and C-H) are coming from the –C(O)OH, C:289.5 eV, O: 532.7 eV and OH: 534.1 eV. In the case of *PNiPAM* [36], the carbon from C-N is found at 286.2 eV, the C=O has position at 288.2 eV for C and 533 eV for the O and finally the N-H is found at 399.2 eV. In the case of the last polymer, *PMETAC*, of more importance is the carbon between the oxygens –O-C(=O)- found at 289 eV and the quaternary N from the R group at 402.8 eV [37]. Here it has to be noted that for

all polymers except the abovementioned peaks, all peaks relevant to C-C and C-H where also used for the calculation of the percentage and the ratios.

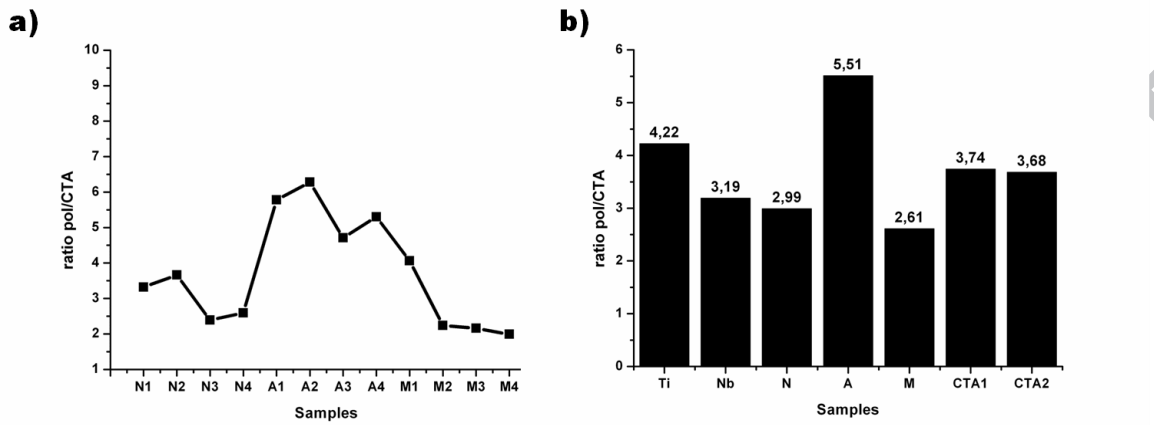


**Figure 2:** a) Ratio of polymer/CTA for all samples calculated via XPS and b) comparison of ratio for different parameters, like i) type of surface, ii) different polymer and iii) concentration of CTA.

In Table 1 the different percentages can be found. The percentages used for C and O where the ones after the integration of the area for the specific peaks. In the case of PNiPAM and PMETAC the N area was also used for the calculation since as can be seen in Table 1 no N was found for PAA. The ratio of polymer/CTA was calculated based on the structure of the monomeric unit of each polymer and the different percentages of C and O (after integration at specific areas), or the N of PNiPAM/PMETAC and the percentages of S/Si (responsible for the CTA structure). The structures of the polymers are: PAA-$C_3O_2$, PNiPAM-$C_6ON$ and PMETAC-$C_9O_2N$. CTA, as already mentioned has 3 S and 1 Si. In Figure 2a it can be seen that based on the ratios polymer/CTA the highest amount of polymer can be found for the sample A2 with a ratio of 6.25 (PAA on $TiO_2$ with 100 mM concentration of CTA) and the lowest on M4 (*PMETAC* on NbO with 100 mM concentration of CTA) with ratio 1.99. Generally, the ratios do not have so big differences among the samples (1.99 to 6.25). In Figure 2a it can be seen that the highest ratio of PAA is found for sample A2 (6.25), for sample N2 (PNiPAM) (3.66) and for sample M1 (PMETAC) (4.06). It can be concluded that the polymerization from $TiO_2$ surfaces is giving higher yields for all homopolymers than in the case of NbO. In Table 1 the percentage of Ti and NbO for all cases is shown. It is found that $TiO_2$ has a median of 15.9 % (11.5-18.6 %) while NbO has 21.1 % (18.2-25.4 %). Also the percentage of N of PNiPAM and PMETAC can be seen, revealing higher percentage in NbO than $TiO_2$ (3.9 vs 2.5 %) and higher percentages of PMETAC than PNiPAM (3.7 vs 2.7%).

Finally, by Figure 2b an interpretation can be derived about how the ratio of polymer/CTA has been influenced based on different parameters such as: i) the metallic surface, ii) the different polymer and iii) the concentration of CTA on the surfaces. Based on that, it is shown that $TiO_2$ is showing higher ratios for the homopolymers with a ratio of 4.22 vs 3.19 for NbO, meaning that the polymers were grafted easier

from $TiO_2$ than from NbO. This is also verified from the higher percentage of CTA (S-Si) that is found in $TiO_2$ (3.62 %) compared to NbO (2.23 %). More probability of polymerization is achieved for higher the percentage of CTA. Among the different polymers, it is evident that PAA is polymerized easier than the other two homopolymers, showing higher ratios of 5.51, while the PNiPAM has 2.99 and PMETAC 2.61. In the case of PMETAC, the concentration of CTA over the metallic surfaces has almost the same ratio for both concentrations (3.74 for 50 mM vs 3.68 for 100 mM), meaning that the polymerization gave almost the same yield. Nevertheless, this does not mean that the coverage and the lengths of the polymer chains is the same. The lowest concentration is more probably due to polymer brushes with higher length but less coverage, so the yield in polymer ratio is almost the same.

### 3.2 AFM

In order to have a visual perspective of the surfaces under different conditions, AFM in dry and liquid state was conducted and the differences in topography and phase were evaluated. The differences of polymer brushes based on different environments can be better monitored in liquid AFM. Initially the surfaces of $TiO_2$ and NbO were characterized without polymers. PNiPAM brushes were also characterized at room temperature. In the case of PMETAC AFM measurements were conducted in dry state. When rinsing the surfaces with water and then with $LiClO_4$, it is expected that the PMETAC will complex with the salt, showing a more hydrophobic behavior [37]. Different pH (4, 7 and 9) conditions were chosen for PAA samples, since PAA is a polyanion that is affected by the differences in pH. In Table 2 are shown the results for the roughness and the median peak of all samples under the different conditions. In Figure 3, 4 and 5 are shown AFM images, in dry state, of polymer brushes of PAA, PMETAC and PNiPAM, respectively. It has to be noted that in the case of PAA and PMETAC it was chosen to present just the case abbreviated with 2; the case with more CTA grafted on the surface. For the rest of the samples it was found that they displayed similar differences in varying pH and ionic strength.

In Figure 3 AFM images in dry state of the sample of A2 ($TiO_2$) (Figure 3 a-d) and A4 (NbO) (Figure 3 e-h) differences can be seen in response to different pH environments. The resulted roughness values for all samples are shown in Table 2. Roughness is enhanced when changing from acidic to basic environments (median change for samples A; from 0.69 nm at pH 4 to 1.66 nm at pH 9 (58 % enhancement)), similarly phase differences are changing from $0.91^o$ to $2.69^o$).

**Table 2:** Results of roughness (nm and $^o$) for dry and liquid measurements from AFM for all samples under different conditions.

| Samples | Roughness (nm) pH (4-7-9) | Roughness (nm) liquid pH (4-7-9) | Roughness ($^o$) pH (4-7-9) | Roughness ($^o$) Liquid pH (4-7-9) |
|---|---|---|---|---|
| **A1** | 1.13-1.72-2.11 (+46%) | - | 1.30-1.78-3.40 | - |

| | | | | |
|---|---|---|---|---|
| **A2** | 0.52-0.85-1.69 (+69%) | 0.95-1.24-1.31 (+27%) | 0.46-1.12-2.18 | 1.49-1.61-2.41 |
| **A3** | 0.50-0.54-0.81 (+38%) | - | 0.78-1.40-1.87 | - |
| **A4** | 0.60-0.73-2.03 (+70%) | 0.66-1.06-1.60 (+59%) | 1.09-1.84-3.31 | 1.05-1.70-2.06 |
| | **Roughness (nm) $H_2O$- $LiClO_4$** | **Roughness (nm) liquid $H_2O$- $LiClO_4$** | **Roughness (°) $H_2O$- $LiClO_4$** | **Roughness (°) Liquid $H_2O$- $LiClO_4$** |
| **M1** | 0.59-1.00 (+41%) | - | 1.89-3.65 | - |
| **M2** | 0.40-1.05 (+62%) | 1.47-2.02 (+27%) | 3.19-4.13 | 1.15-2.46 |
| **M3** | 0.57-2.32 (+75%) | - | 1.75-4.20 | - |
| **M4** | 0.34-1.72 (+80%) | 1.22-1.83 (+33%) | 2.38-3.05 | 3.30-4.39 |
| | **Roughness (nm)** | | **Roughness (°)** | |
| **N1** | 0.94 | | 1.85 | |
| **N2** | 1.04 | | 1.31 | |
| **N3** | 0.34 | | 0.26 | |
| **N4** | 0.83 | | 1.21 | |

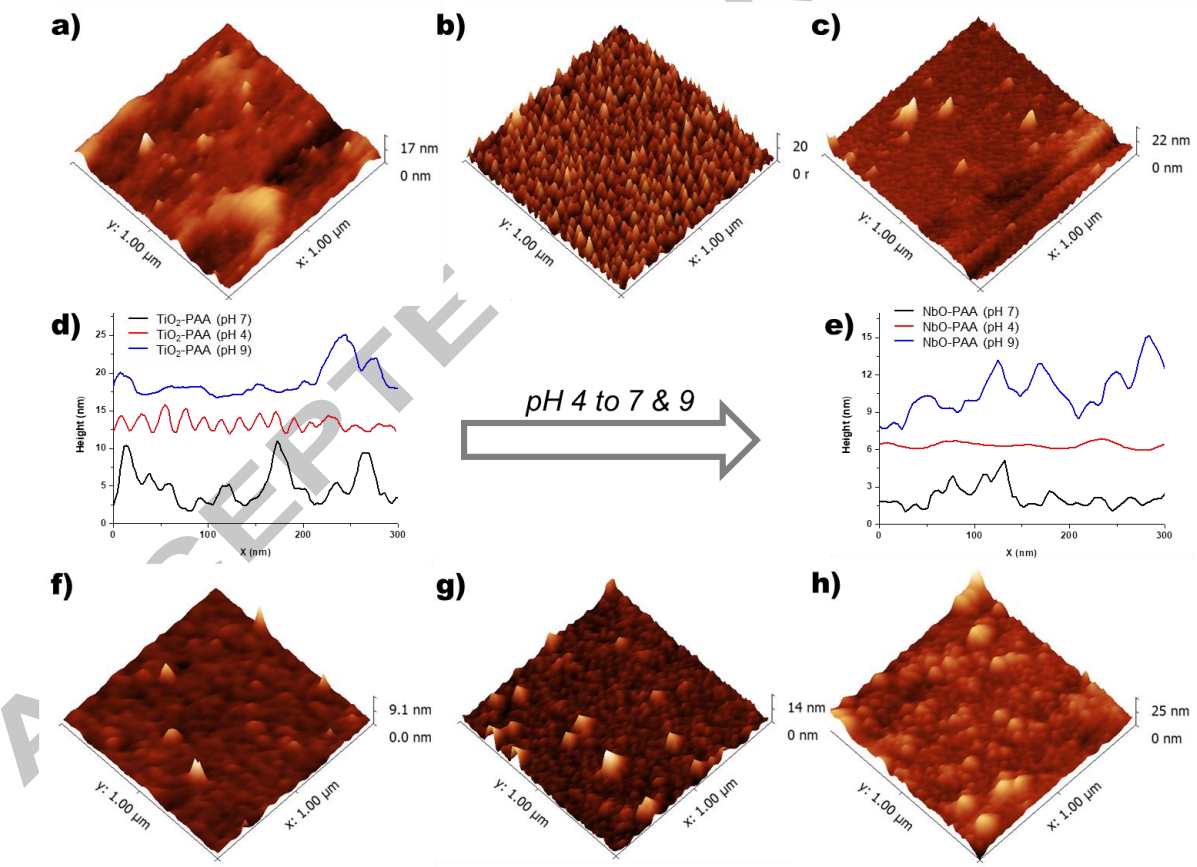


**Figure 3:** AFM images of the height in dry state 1µm x 1 µm. Representation of topography changes at different pH values of sample A2 ($TiO_2$) at a) pH 4, b) pH 7 and c) pH 9 and of sample A4 (NbO) at f) pH 4, g) pH 7 and h) pH 9. Cut sections of 300 nm of d) $TiO_2$ and e) NbO.

It is well known as reported elsewhere [4,38,39] that by increasing the pH the height of the PAA brushes is enhanced, since coulombic repulsions are forcing the polymer chains to adopt an extent conformation; when changing from acidic environments and coil conformations, the chains are changing to stretched conformations in basic environments. The latter is verified by the topography and phase changes of all samples with PAA after exposing them at different pH values, as well as, by the profiles cut sections as can be seen in the interior images of Figure 3. In Figure 3 no big agglomerations can be distinguished, although it is clear that the topography is changing by altering the pH of the environment, even in dry state.

In Figure 4 AFM images of PMETAC grafted from $TiO_2$/NbO can be seen for sample M2 ($TiO_2$) (Figure 4 a,b) and B4 (NbO) (Figure 4 c,d), before and after treatment with $LiClO_4$. As already mentioned above it is well established that the $LiClO_4$ can complex with the quaternary amines of PMETAC, creating a more hydrophobic surface. Roughness results are presented in Table 2 and in Figure 4 it is shown the initial hypothesis. The topography of M2 after treatment with this salt is showing higher agglomerations not only in height (samples M changing their roughness from 0.48 nm to 1.52 nm, 68% enhancement) but also in phase ($2.30^o$ to $3.76^o$). In the profile cut sections it is also clear that after the salt addition the surface becomes rougher and PMETAC chains are creating agglomerations. In Table 2 are shown changes in roughness for height and phase.

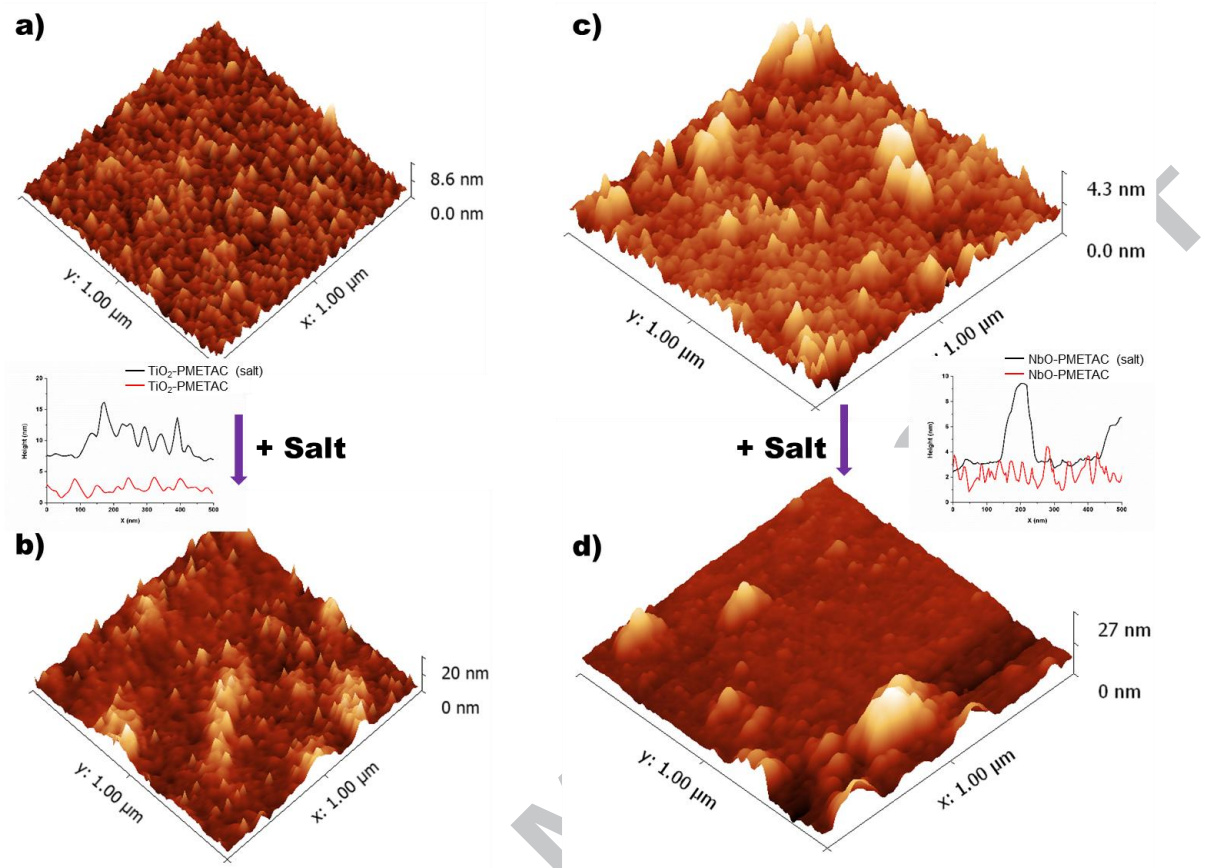


**Figure 4:** AFM images in dry state for the responsiveness of PMETAC with salt treatment, a) M2 ($TiO_2$) 1 µm x 1 µm (height) without treatment, b) M2 (M2) 1 µm x 1 µm (height) after $LiClO_4$ treatment, c) M4 (NbO) 1 µm x 1 µm (height) without treatment, d) M4 (NbO) 1 µm x 1 µm (height) after $LiClO_4$ treatment. Profiles of 500 nm can be seen as inner images.

In Figure 5 AFM images of all samples with PNiPAM can be seen. Topography and roughness of PNiPAM brushes found to be similar to PNiPAM brushes [18]. Samples with more concentration of CTA have yield in more polymer brushes, as rougher topography can be seen (comparing Figure 5a with b and c with d). By comparing the surfaces in terms of roughness based on the different polymers on the surface in dry state without any treatment, it can be found that the samples with PMETAC display the lowest roughness 0.48 nm. In addition, samples with PNiPAM show roughness of 0.79 nm and with PAA 0.96 nm. Comparing the phase differences the more homogeneous surface was found to be the one with PNiPAM (1.16$^o$), PAA has a phase difference of 1.54$^o$ and PMETAC 2.30$^o$.

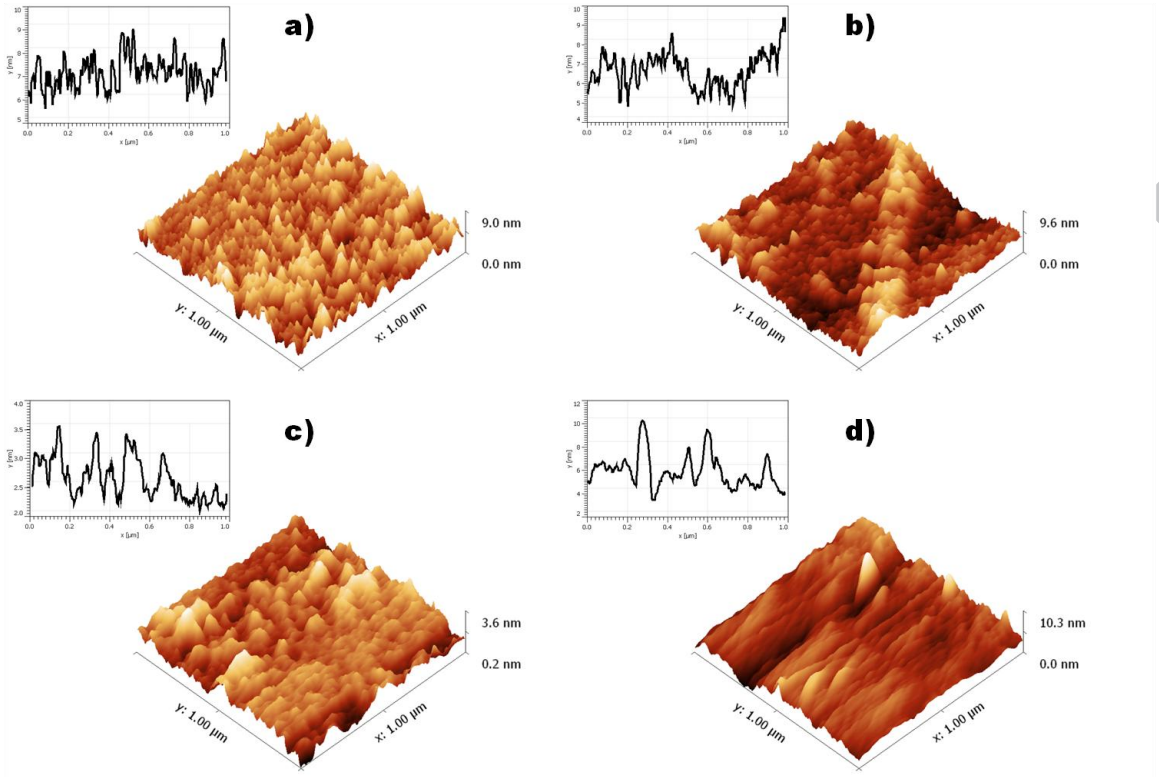


**Figure 5:** AFM images in dry state for a) N1 ($TiO_2$) 1 µm x 1 µm (height), b) N2 ($TiO_2$) 1 µm x 1 µm (height), c) N3 (NbO) 1 µm x 1 µm (height) and d) N4 (NbO) 1 µm x 1 µm (height). Inner images; profiles cut section for 1 µm.

Roughness of $TiO_2$ surfaces with the different polymers is 0.77 nm while in the case of NbO surfaces with the same polymers is 0.56 nm. Evaluating each metallic surface and polymer it can be found how roughness is altered depending on the sample. $TiO_2$-PAA samples display enhanced roughness from pH 4 to pH 9 (0.83 to 1.90 nm)-(56 %) while NbO-PAA samples have less roughness but higher enhancement (0.55 to 1.42 nm)-(61 %). Similarly, samples of $TiO_2$-PMETAC have enhanced roughness with the addition of salt (0.50 to 1.25 nm)-(60 %) while samples of NbO-PMETAC have higher values of roughness and more increased percentage (0.46 to 2.02 nm)-(77 %). Those differences and the increment in percentage can be seen in Table 2. Samples with PAA show an increase from 38 to 70 %, with A4 displaying the higher increase. PMETAC samples increase from 41 to 80 %, with M4 showing the higher increase.

In liquid AFM the solution was changed in situ varying the pH or the ionic strength and measure the response of the polymer brush in each case, in terms of topography and roughness as can be seen in Figure 6 and 7.

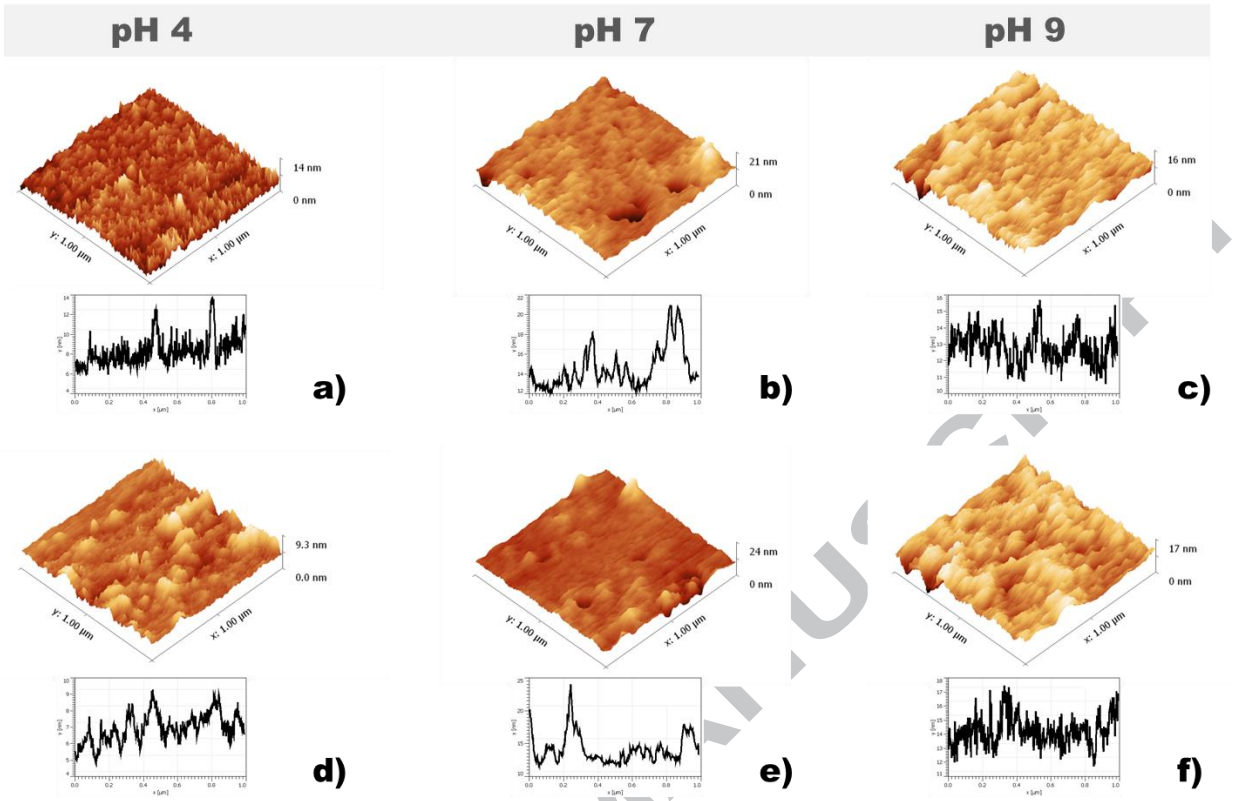


**Figure 6:** AFM images in liquid of 1 µm x 1 µm (height) for PAA samples a) A2 pH 4, b) A2 pH 7, c) A2 pH 9, d) A4 pH 4, e) A4 pH 7 and f) A4 pH 9. As interior images the phase and profile cut section of 1µm can be seen.

In Figure 6 can be seen the differences in topography by changing the pH, for samples with PAA-A2 and A4. The differences in topography, by changing the ionic strength, are shown in Figure 7 for PMETAC-M2 and M4 samples. Cut sections and phase images can be also found in Figure 6 and 7. Monitoring the roughness, it is clear that the change in pH or ionic strength can be crucial affecting significantly the physicochemical properties of the surface. PAA samples display an enhancement of roughness from 0.81 nm to 1.46 nm ($1.27^{o}$ to $2.24^{o}$)-(45 %). The increase in roughness of A2 is 27 % and that of A4 59 %. PMETAC samples show smaller changes but quite evident, with enhancement from 1.35 nm to 1.93 nm ($2.23^{o}$ to $3.43^{o}$)-(30 %), with the increase of M2 being 27 % and that of M4 33 %. Comparing the surfaces in liquid, $TiO_2$ has a median roughness of 1.21 nm while NbO has 0.94 nm. The differences in topography in these surfaces can be controlled with different polymer brushes grafted from the surface while varying the concentration of CTA the grafting density can also be affected, showing different roughness.

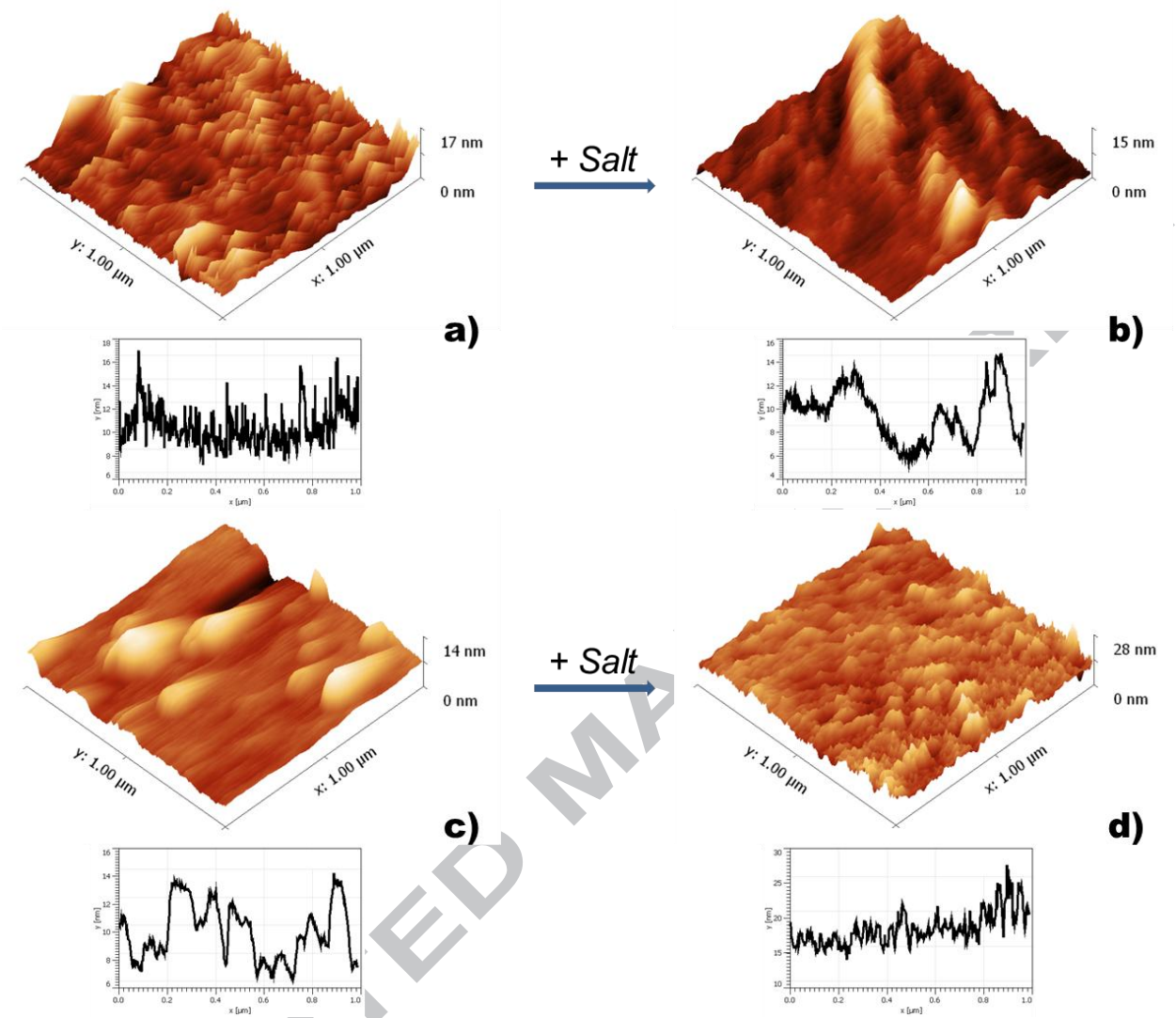


**Figure 7:** AFM images in liquid of 1 µm x 1 µm (height) for PMETAC samples a) M2 without $LiClO_4$, b) M2 with $LiClO_4$, c) M4 without $LiClO_4$ and d) M4 with $LiClO_4$. As interior images the phase and profile cut section of 1µm can be seen.

### 3.3 Contact Angle

The switching behavior of the polymer brushes grafted from $TiO_2$ and NbO was also evaluated by means of contact angle. Besides the differences in height, topography and roughness shown via for the different samples it is possible to evaluate their responsiveness in different conditions via contact angle measurements.

In Table 3 can be seen contact angle values for all samples of $TiO_2$ and NbO surfaces. Measurements in samples of PAA were conducted at three different pH values (4, 7 and 9), PNiPAM at lower and higher temperatures than the switching temperature for the conformational change for PNiPAM and for PMETAC before and after treatment with $LiClO_4$ (45 °C to 20 °C).

**Table 3:** Contact angle values for all polymers grafted from $TiO_2$ & NbO under different environments, showing their responsiveness.

| Samples | 45°C | 20°C | Samples | pH 4 | pH 7 | pH 9 | Samples | pH 7 | salt |
|---|---|---|---|---|---|---|---|---|---|
| **N1($TiO_2$)** | 58.5 | 49.0 | **A1($Ti O_2$)** | 96.6 | 62.0 | 56.0 | **M1($Ti O_2$)** | 32.8 | 37.0 |
| **N2($Ti O_2$)** | 52.0 | 25.8 | **A2($Ti O_2$)** | 68.0 | 55.0 | 47.0 | **M2($Ti O_2$)** | 31.5 | 49.7 |
| **N3(NbO)** | 48.0 | 32.0 | **A3(NbO)** | 80.0 | 72.0 | 62.0 | **M3(NbO)** | 20.0 | 34.3 |
| **N4(NbO)** | 43.3 | 31.0 | **A4(NbO)** | 64.0 | 54.0 | 46.0 | **M4(NbO)** | 22.7 | 45.4 |
| **Difference** | 32% | | **Difference** | 31% | | | **Difference** | 35% | |

In the case of PNiPAM brushes the changes on the conformation of the chains is based in alteration of the temperature. At temperatures higher than 32 °C the PNiPAM brushes become more hydrophobic due to changes in conformations. The contact angle values for both surfaces can be seen in Table 3 and Figure 8a at 20 °C and at 45 °C. The biggest changes can be found for the N2 sample (52.0 to 25.8 -50 %). For $TiO_2$ the changes are 33.0 % and for the NbO 30.5. Different concentrations of CTA show difference of 24.5% and 39 % for 50 mM and 100 mM, respectively.

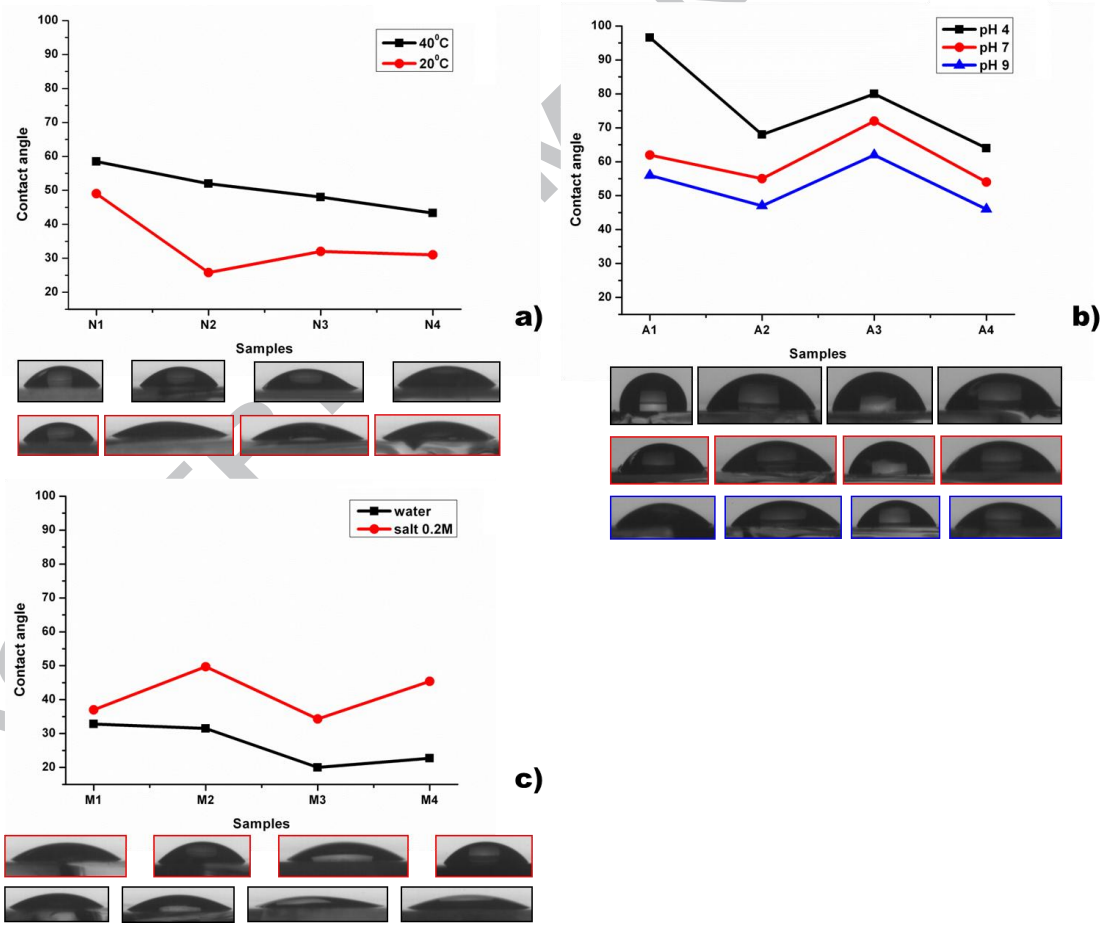


**Figure 8:** Contact angle photos and graphs, showing the differences in wetting of surfaces for a) different temperature PNiPAM samples (N1-N4), b) different pH PAA samples (A1-A4) and c) different ionic strength PMETAC samples (M1-M4).

In Table 3 and Figure 8b, it can be seen that for all surfaces with PAA when changing the pH from acidic to basic the surface is becoming more hydrophilic. Results showed different response based on the concentration of the CTA and subsequently of the yield of polymers and on the type of metallic surface. The biggest difference is 42% for sample A1, changing from 96.6 to 62.0, while at pH 9 to 56.0 the difference was 42 %. The more increased hydrophilic behavior at basic environments is due to the fact that the higher the pH the higher the electric charge, from the electrostatic repulsion of the neighbor negatively charged PAA groups, leading to a more hydrophilic behavior [39,40]. The switching behavior from acidic to basic environment for both surfaces found to be 36.5% more hydrophilic for $TiO_2$ and 25.5 % more hydrophilic for NbO surfaces. Concerning the different CTA concentrations at 50 mM (samples 1 and 3) show differences of 32.5 %, while at 100 mM (samples 2 and 4) show changes of 29. 5 %.

Finally, in the case of PMETAC, after treatment with $LiClO_4$ the surfaces are becoming more hydrophobic due to the complexing of the quaternary amino groups of the PMETAC with salt. In Table 3 and Figure 8c the hydrophobic behavior after salt treatment can be seen. The bigger difference is 50 % and can be seen for sample M4 (changing from 45.4 to 22.7). The switching behavior for both surfaces was found to be 24.0 % for $TiO_2$ and 46.0 % for NbO surfaces. Different concentrations of CTA; 50 mM and 100 mM showed differences of 26.5 % and 43.5 % respectively.

Generally, the changes found in contact angle values are from 25.8 to 58.5 for PNiPAM with differences of 32 %, from 46.0 to 96.6 for PAA with differences of 31 % and finally from 20 to 49.7 for PMETAC with differences of 35 %.

### 3.4 Confocal Measurements

In order to visualize cell adhesion on the $TiO_2$ surfaces functionalized with polymer brushes; PAA, PNiPAM and PMETAC, MC-3-T3 cells were cultured for 24 hours. F-actin staining, presented in red color at the left side column in Figures 9-12, provide information related to the size and population of the cells while the orientation, extension and diffusion of the stress fibers over the cytoplasm can also be evaluated. Vinculin protein, presented with green color, connects the stress fibers with the membrane at the sites of cell anchorage providing information related to the focal adhesion of the cells to the surface. On the right column of Figures 9-12 is presented the merged image of F-actin, Vinculin and nucleous staining. Cell adhesion on $TiO_2$ and NbO surfaces without polymer brushes were studded as a control (Figure 9). Cells were well spread and migrated in both control samples of $TiO_2$ and NbO as can be distinguished in Figure 9. Both samples displayed well-defined and extended stress fibers as observed by F-actin staining, while the focal contact points of Vinculin staining, displayed as bright spots, were extended all over the surface of the cell anchorage.

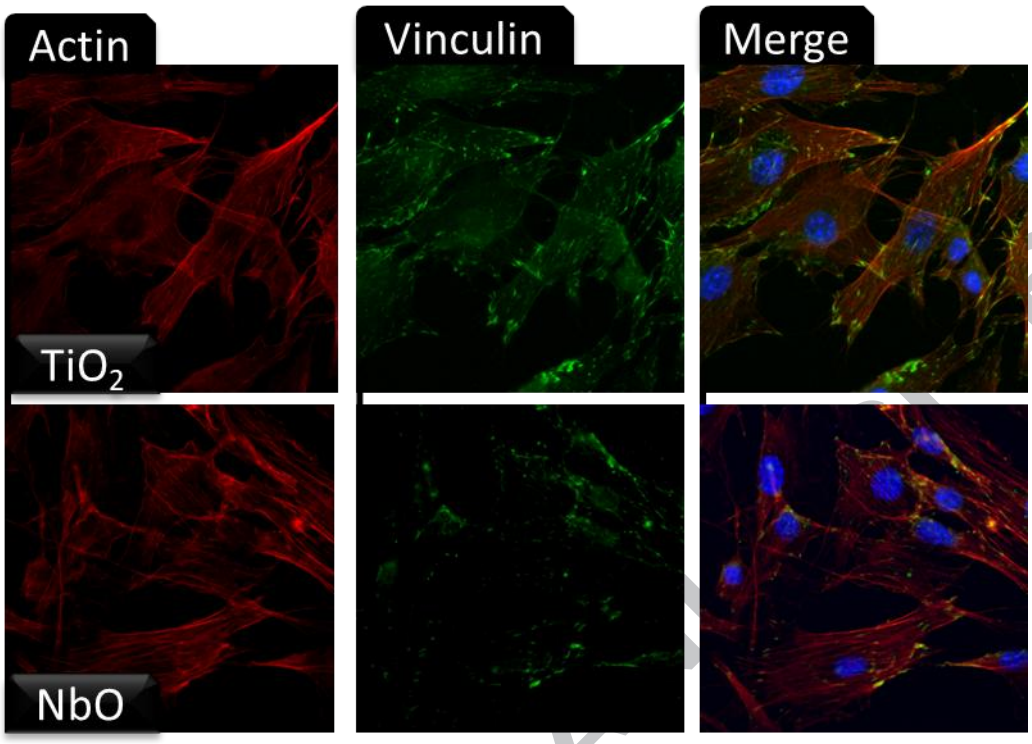


**Figure 9:** Confocal scanning laser microscopy images of stained MC-3-T3 cells seeded for 24 hours for focal adhesion studies on top of $TiO_2$ and NbO surfaces. Scale for all images was 20 μm.

In Figure 10 samples A1-4 showed consistent cell growth that had also well-defined and extended stress fibers all over the treated surfaces. In addition, they presented several focal contacts per cell, hinting biocompatible surfaces. On the other hand, sample A4 showed a limited cell growth; even though the cells were well spread with high fluorescence intensity focal contact points, they did not proliferate as in the other three samples.

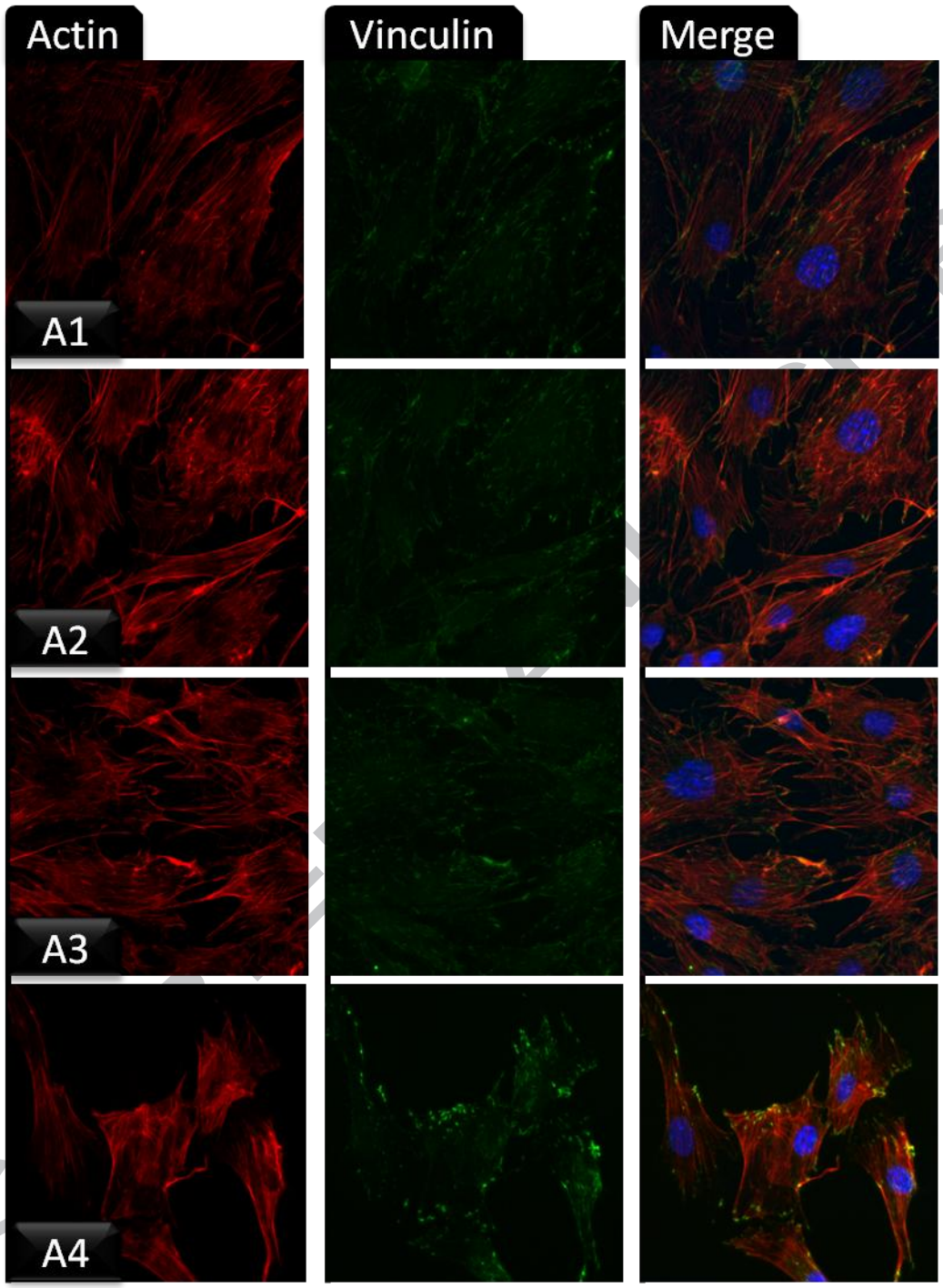


**Figure 10:** Confocal scanning laser microscopy images of stained MC-3-T3 cells seeded for 24 hours for focal adhesion studies on top of $TiO_2$ and NbO surfaces functionalized with PAA. Scale for all images was 20 μm.

The cells in samples presented in Figure 11 were well diffused forming a fine cell matrix over the PMETAC brushes. The focal adhesion points in samples M1, M2, M3 and M4 were pronounced, revealing good cellular adhesion and proliferation. Samples in Figure 12 showed also good cellular focal

adhesion although in the case of sample N1, N2 and N3 the cells seemed to be adhered onto less smooth surfaces as the stress fibers are folded as seen for instance in the case of sample N1 and N2.

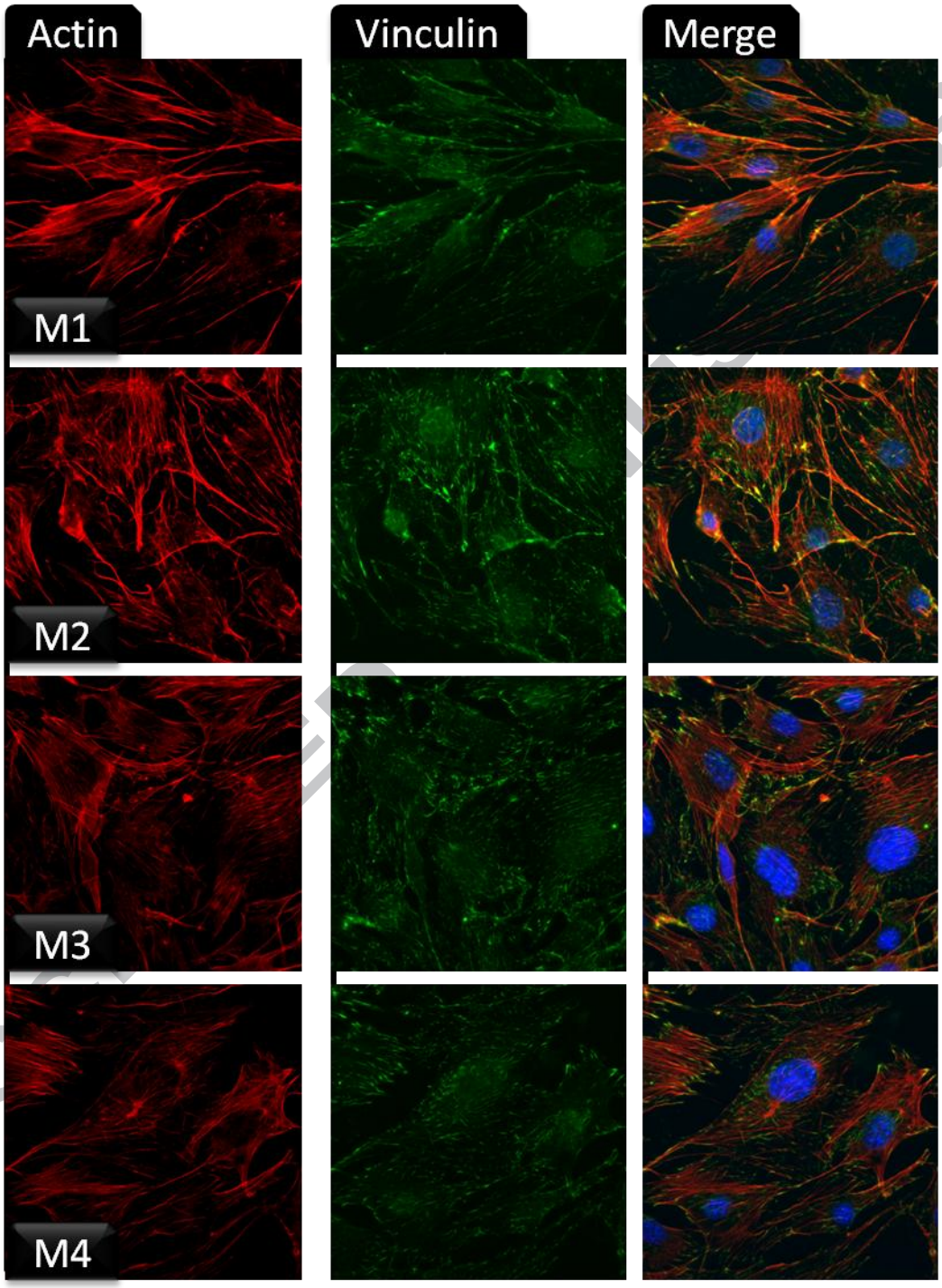


**Figure 11:** Confocal scanning laser microscopy images of stained MC-3-T3 cells seeded for 24 hours for focal adhesion studies on top of $TiO_2$ and NbO surfaces functionalized with PMETAC. Scale for all images was 20 µm.

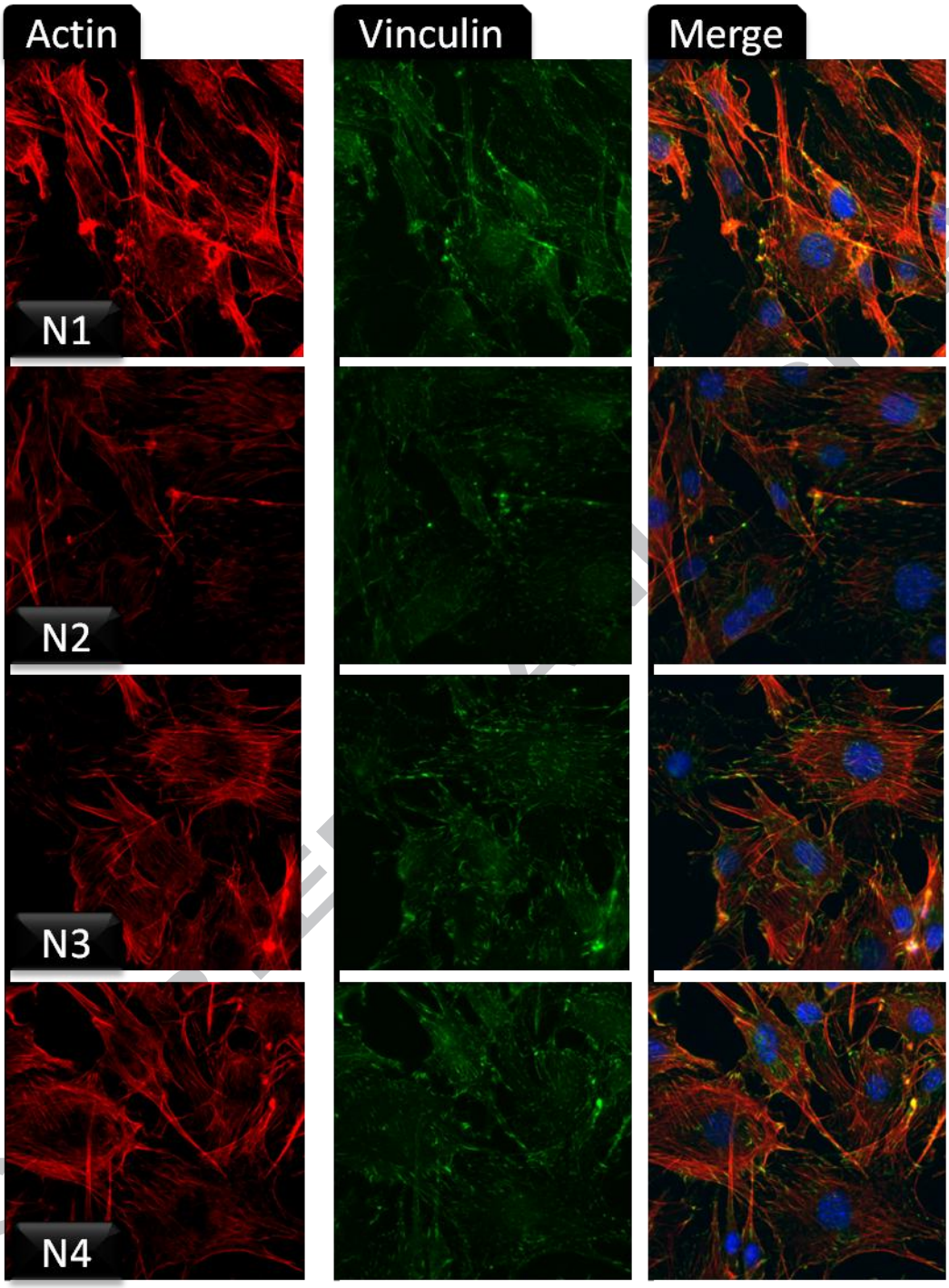


**Figure 12:** Confocal scanning laser microscopy images of stained MC-3-T3 cells seeded for 24 hours for focal adhesion studies on top of $TiO_2$ and NbO surfaces functionalized with PNIPAm. Scale for all images was 20 μm.

In conclusion, functionalized surfaces with PAA resulted in more elevated focal adhesion comparing to the other functionalized surfaces. As a proof of concept all three of them showed satisfactory results in terms of biocompatibility.

## 4. Conclusions

The surfaces of $TiO_2$ and NbO oxides with polymer brushes grafting from them were examined. The use of three different polymers with switchable behavior in external stimulus was confirmed from contact angle and AFM in dry and liquid state. It was shown that in the case of the pH sensitive PAA, changes of pH could alter its physicochemical properties such as the height of the brushes and their hydrophilicity. PNiPAM is a thermoresponsive polymer that reacts with temperature alterations as shown in contact angle measurements. Moreover, PMETAC is a positively charged polyelectrolyte that can change its hydrophobicity in relation to different salts and ionic strength. The use of these responsive polymers in combination with metallic surfaces that are known for their good biocompatible and mechanical properties led to smart material surfaces that can be used in different kind of biomedical applications. The synthesis of the polymer brushes was evaluated through XPS measurements, showing the ratio of the polymer brushes in respect of each surface. Confocal experiments showed enhanced growth of cells after 24 hours in all cases with polymer brushes, when compared to bare $TiO_2$ or NbO surfaces. Biocompatibility of the polymer brushes over $TiO_2$ or NbO surfaces can be of great importance and potentially play a key role for the use of responsive polymeric surfaces in biological applications.

**Author Agreement/Declaration:** All authors have seen and approved the final version of the manuscript being submitted.

**Conflict of Interest:** All authors declare that they do not have any conflict of interest.

**Data Availability Statement**: The raw/processed data required to reproduce these findings cannot be shared at this time due to technical or time limitations.

**References**

[1] S. Peng, B. Bhushan, Smart polymer brushes and their emerging applications, RSC Adv. 2 (2012) 8557. doi:10.1039/c2ra20451g.

[2] S. Edmondson, V.L. Osborne, W.T.S. Huck, Polymer brushes via surface-initiated polymerizations, Chem. Soc. Rev. 33 (2004) 14. doi:10.1039/b210143m.

[3] M. Ramstedt, N. Cheng, O. Azzaroni, D. Mossialos, H.J. Mathieu, W.T.S. Huck, Synthesis and characterization of poly(3-sulfopropylmethacrylate) brushes for potential antibacterial applications, Langmuir. 23 (2007) 3314–3321. doi:10.1021/la062670+.

[4] N. Ayres, S.G. Boyes, W.J. Brittain, Stimuli-Responsive Polyelectrolyte Polymer Brushes Prepared via Atom-Transfer Radical Polymerization †, Langmuir. 23 (2007) 182–189. doi:10.1021/la061526l.

[5] P. Ye, H. Dong, M. Zhong, K. Matyjaszewski, Synthesis of Binary Polymer Brushes via Two-Step Reverse Atom Transfer Radical Polymerization, Macromolecules. 44 (2011) 2253–2260. doi:10.1021/ma1028533.

[6] P.M. Mendes, Stimuli-responsive surfaces for bio-applications, Chem. Soc. Rev. 37 (2008) 2512. doi:10.1039/b714635n.

[7] O. Azzaroni, Polymer brushes here, there, and everywhere: Recent advances in their practical applications and emerging opportunities in multiple research fields, J. Polym. Sci. Part A Polym. Chem. 50 (2012) 3225–3258. doi:10.1002/pola.26119.

[8] M. Zamfir, C. Rodriguez-Emmenegger, S. Bauer, L. Barner, A. Rosenhahn, C. Barner-Kowollik, Controlled growth of protein resistant PHEMA brushes via S-RAFT polymerization, J. Mater. Chem. B. 1 (2013) 6027. doi:10.1039/c3tb20880j.

[9] J. Choi, P. Schattling, F.D. Jochum, J. Pyun, K. Char, P. Theato, Functionalization and patterning of reactive polymer brushes based on surface reversible addition and fragmentation chain transfer polymerization, J. Polym. Sci. Part A Polym. Chem. 50 (2012) 4010–4018. doi:10.1002/pola.26200.

[10] D.J. Keddie, A guide to the synthesis of block copolymers using reversible-addition fragmentation chain transfer (RAFT) polymerization, Chem. Soc. Rev. 43 (2014) 496–505. doi:10.1039/C3CS60290G.

[11] M.H. Stenzel, L. Zhang, W.T.S. Huck, Temperature-Responsive Glycopolymer Brushes Synthesized via RAFT Polymerization Using the Z-group Approach, Macromol. Rapid

Commun. 27 (2006) 1121–1126. doi:10.1002/marc.200600223.

[12] B.A. Rozenberg, R. Tenne, Polymer-assisted fabrication of nanoparticles and nanocomposites, Prog. Polym. Sci. 33 (2008) 40–112. doi:10.1016/j.progpolymsci.2007.07.004.

[13] Y. Xu, A. Walther, A.H.E. Müller, Direct Synthesis of Poly(potassium 3-sulfopropyl methacrylate) Cylindrical Polymer Brushes via ATRP Using a Supramolecular Complex With Crown Ether, Macromol. Rapid Commun. 31 (2010) 1462–1466. doi:10.1002/marc.201000157.

[14] W.K. Cho, B. Kong, H.J. Park, J. Kim, W. Chegal, J.S. Choi, et al., Long-term stability of cell micropatterns on poly((3-(methacryloylamino)propyl)-dimethyl(3-sulfopropyl)ammonium hydroxide)-patterned silicon oxide surfaces, Biomaterials. 31 (2010) 9565–9574. doi:10.1016/j.biomaterials.2010.08.037.

[15] M. Kobayashi, M. Terada, A. Takahara, Reversible adhesive-free nanoscale adhesion utilizing oppositely charged polyelectrolyte brushes, Soft Matter. 7 (2011) 5717. doi:10.1039/c1sm05132f.

[16] Y.K. Jhon, R.R. Bhat, C. Jeong, O.J. Rojas, I. Szleifer, J. Genzer, Salt-Induced Depression of Lower Critical Solution Temperature in a Surface-Grafted Neutral Thermoresponsive Polymer, Macromol. Rapid Commun. 27 (2006) 697–701. doi:10.1002/marc.200600031.

[17] A. Mizutani, A. Kikuchi, M. Yamato, H. Kanazawa, T. Okano, Preparation of thermoresponsive polymer brush surfaces and their interaction with cells, Biomaterials. 29 (2008) 2073–2081. doi:10.1016/j.biomaterials.2008.01.004.

[18] N. Idota, A. Kikuchi, J. Kobayashi, K. Sakai, T. Okano, Modulation of graft architectures for enhancing hydrophobic interaction of biomolecules with thermoresponsive polymer-grafted surfaces, Colloids Surfaces B Biointerfaces. 99 (2012) 95–101. doi:10.1016/j.colsurfb.2011.10.033.

[19] N. Huang, R. Michel, J. Voros, M. Textor, R. Hofer, A. Rossi, et al., Poly ( L -lysine ) - g -Poly ( ethylene glycol ) Layers on Metal Oxide Surfaces : Surface-Analytical Character Adsorption †, Langmuir. 17 (2001) 489–498. http://pubs.acs.org/doi/pdf/10.1021/la000736+.

[20] B. Pidhatika, M. Rodenstein, Y. Chen, E. Rakhmatullina, A. Mühlebach, C. Acikgöz, et al., Comparative Stability Studies of Poly(2-methyl-2-oxazoline) and Poly(ethylene

glycol) Brush Coatings, Biointerphases. 7 (2012) 1. doi:10.1007/s13758-011-0001-y.

[21] M. Charnley, M. Textor, C. Acikgoz, Designed polymer structures with antifouling–antimicrobial properties, React. Funct. Polym. 71 (2011) 329–334. doi:10.1016/j.reactfunctpolym.2010.10.013.

[22] B. Malisova, S. Tosatti, M. Textor, K. Gademann, S. Zürcher, Poly(ethylene glycol) Adlayers Immobilized to Metal Oxide Substrates Through Catechol Derivatives: Influence of Assembly Conditions on Formation and Stability, Langmuir. 26 (2010) 4018–4026. doi:10.1021/la903486z.

[23] B. Pidhatika, J. Möller, E.M. Benetti, R. Konradi, E. Rakhmatullina, A. Mühlebach, et al., The role of the interplay between polymer architecture and bacterial surface properties on the microbial adhesion to polyoxazoline-based ultrathin films, Biomaterials. 31 (2010) 9462–9472. doi:10.1016/j.biomaterials.2010.08.033.

[24] S. Pasche, S.M. De Paul, J. Vörös, N.D. Spencer, M. Textor, Poly( <scp>l</scp> -lysine)-*g raft* -poly(ethylene glycol) Assembled Monolayers on Niobium Oxide Surfaces: A Quantitative Study of the Influence of Polymer Interfacial Architecture on Resistance to Protein Adsorption by ToF-SIMS and in Situ, Langmuir. 19 (2003) 9216–9225. doi:10.1021/la034111y.

[25] F. Variola, F. Vetrone, L. Richert, P. Jedrzejowski, J.-H. Yi, S. Zalzal, et al., Improving Biocompatibility of Implantable Metals by Nanoscale Modification of Surfaces: An Overview of Strategies, Fabrication Methods, and Challenges, Small. 5 (2009) 996–1006. doi:10.1002/smll.200801186.

[26] G. Ramírez, S.E. Rodil, H. Arzate, S. Muhl, J.J. Olaya, Niobium based coatings for dental implants, Appl. Surf. Sci. 257 (2011) 2555–2559. doi:10.1016/j.apsusc.2010.10.021.

[27] B. O'Brien, W. Carroll, The evolution of cardiovascular stent materials and surfaces in response to clinical drivers: A review, Acta Biomater. 5 (2009) 945–958. doi:10.1016/j.actbio.2008.11.012.

[28] H. Zitter, H. Plenk, The electrochemical behavior of metallic implant materials as an indicator of their biocompatibility, J. Biomed. Mater. Res. 21 (1987) 881–896. doi:10.1002/jbm.820210705.

[29] H. Matsuno, A. Yokoyama, F. Watari, M. Uo, T. Kawasaki, Biocompatibility and osteogenesis of refractory metal implants, titanium, hafnium, niobium, tantalum and

rhenium., Biomaterials. 22 (2001) 1253–62. http://www.ncbi.nlm.nih.gov/pubmed/11336297.

[30] X. Fan, L. Lin, P.B. Messersmith, Cell Fouling Resistance of Polymer Brushes Grafted from Ti Substrates by Surface-Initiated Polymerization: Effect of Ethylene Glycol Side Chain Length, Biomacromolecules. 7 (2006) 2443–2448. doi:10.1021/bm060276k.

[31] J.E. Raynor, T.A. Petrie, K.P. Fears, R.A. Latour, A.J. García, D.M. Collard, Saccharide Polymer Brushes To Control Protein and Cell Adhesion to Titanium, Biomacromolecules. 10 (2009) 748–755. doi:10.1021/bm8011924.

[32] F. Zhang, F.J. Xu, E.T. Kang, K.G. Neoh, Modification of Titanium via Surface-Initiated Atom Transfer Radical Polymerization (ATRP), Ind. Eng. Chem. Res. 45 (2006) 3067–3073. doi:10.1021/ie051225r.

[33] Q. Yu, Y. Zhang, H. Wang, J. Brash, H. Chen, Anti-fouling bioactive surfaces, Acta Biomater. 7 (2011) 1550–1557. doi:10.1016/j.actbio.2010.12.021.

[34] R. Barbey, L. Lavanant, D. Paripovic, N. Schüwer, C. Sugnaux, S. Tugulu, et al., Polymer Brushes via Surface-Initiated Controlled Radical Polymerization: Synthesis, Characterization, Properties, and Applications, Chem. Rev. 109 (2009) 5437–5527. doi:10.1021/cr900045a.

[35] P. Louette, F. Bodino, J.-J. Pireaux, Poly(acrylic acid) (PAA) XPS Reference Core Level and Energy Loss Spectra, Surf. Sci. Spectra. 12 (2005) 22–26. doi:10.1116/11.20050905.

[36] E.C. Cho, Y.D. Kim, K. Cho, Thermally responsive poly(N-isopropylacrylamide) monolayer on gold: synthesis, surface characterization, and protein interaction/adsorption studies, Polymer (Guildf). 45 (2004) 3195–3204. doi:10.1016/j.polymer.2004.02.052.

[37] N. Politakos, S. Azinas, S.E. Moya, Responsive Copolymer Brushes of Poly[(2-(Methacryloyloxy)Ethyl) Trimethylammonium Chloride] (PMETAC) and Poly( 1 H, 1 H, 2 H, 2 H-Perfluorodecyl acrylate) (PPFDA) to Modulate Surface Wetting Properties, Macromol. Rapid Commun. 37 (2016) 662–667. doi:10.1002/marc.201500630.

[38] J. Wang, P. Somasundaran, Reversible conformational behavior of poly(acrylic acid) LB film with changes in pH, ionic strength and time, Colloids Surfaces A Physicochem. Eng. Asp. 273 (2006) 63–69. doi:10.1016/j.colsurfa.2005.08.016.

[39] E. Bittrich, M. Kuntzsch, K.-J. Eichhorn, P. Uhlmann, Complex pH- and temperature-sensitive swelling behavior of mixed polymer brushes, J. Polym. Sci. Part B Polym. Phys.

48 (2010) 1606–1615. doi:10.1002/polb.22021.

[40] H. Almeida, M.H. Amaral, P. Lobão, Temperature and pH stimuli-responsive polymers and their applications in controlled and selfregulated drug delivery, J. Appl. Pharm. Sci. 2 (2012) 01-10. doi:10.7324/JAPS.2012.2609.

Graphical abstract

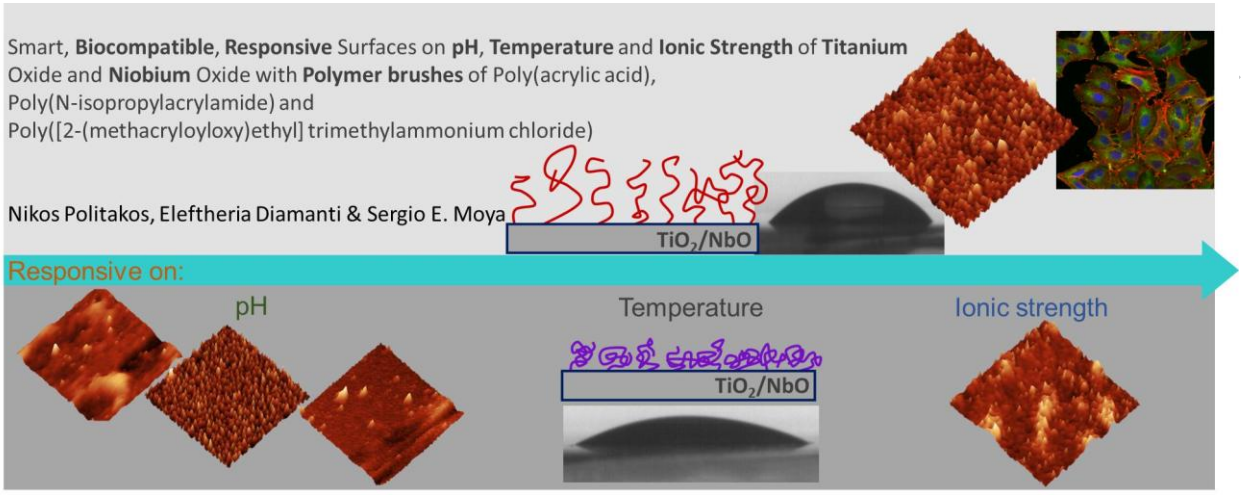

**Highlights**

- Responsive polymer brushes grafted from $TiO_2$ and NbO surfaces
- AFM (liquid-dry) and contact angle characterization to show responsiveness
- Responsive to pH, ionic strength and temperature
- Increased biocompatibility of preosteoblasts at polymer brushes samples
- Confocal microscopy reveals cellular adhesion